Numerical Simulation on Spray Characteristics of Fuel Jet in a Crossflow

*MEI Yu, ZHANG Ping, YAN Yingwen**

College of Energy and Power Engineering, Nanjing University of Aeronautics and Astronautics, Nanjing 210016, P.R. China

(Received 24 May 2020; revised 7 September 2020; accepted 17 September 2020)

Abstract: Spray performance downward the plain orifice injector was numerically simulated by using Fluent. The primary breakup and the secondary breakup were both focused. To capture the instantaneous interface of two-phase flow and multiscale structure of liquid spray more accurately, an adaptive mesh refinement (AMR) method was adopted. Firstly, the velocity distribution and jet structure were obtained. Then, with different coupled VOF (Volume of Fluid)-DPM (Discrete Phase model) strategies, the jet trajectory, the column breakup point, and the time-average SMD distribution were analyzed and compared. Meanwhile, the experimental data and several empirical formulas were applied to verify the numerical value. The results suggested that the numerical simulation could accord well with experimental data and a certain formula.

Key words: plain orifice injector; primary breakup; secondary breakup; jet trajectory; SMD

CLC number: V231.2 **Document code**: A **Article ID**: 1005-1120(2020)S-0018-10

0 Introduction

The kerosene is generally injected from the plain orifice injector as a round jet in a crossflow. The liquid jet undergoes both the effects of liquid viscous force and gas aerodynamic force, which results in the jet breaking into small liquid structures and further disintegrating into droplets. The atomization process is divided into two stages: primary breakup and secondary breakup. The primary breakup firstly occurs in the vicinity of the injection exit[1].

In the primary breakup stage, the shear force generated by the air-fuel interaction leads to the longitudinal instability of the liquid surface, and a sinusoidal global oscillation occurs along the flow direction, which causes the liquid surface breaking into a liquid film or liquid strip[2-3].

Subsequently, there is the secondary breakup. In this stage, these film and band structures fluctuate laterally and continue to split into small droplets. The atomization process involves multi-scale structures, abrupt changes in physical quantity (density, viscosity) which make it difficult to simulate the whole process of atomization accurately.

In current researches most of them applied different solvers and methods to simulate the primary breakup and secondary breakup processes respectively. Brinckman et al.[4] summarized the Computational fluid dynamics (CFD) method for liquid jet atomization, and mentioned that the current engineering model for the primary atomization of liquid jets is progressing well. The engineering model can predict the local rate of droplet formation and their sizes along a gas/liquid interface. And then by combining the discrete phase model, the whole process of liquid jet atomization (from liquid jet breakup/atomization to droplet vaporization) was analyzed, which was shown in Fig.1.

In the primary breakup stage, Ménard et al.[5] carried out numerical simulations to describe the dense zone of a spray where very little information is available. Interface tracking is ensured by the level set method and the ghost fluid method (GFM) is used to capture accurately sharp disconti-

*Corresponding author, E-mail address: yanyw@nuaa.edu.cn.

How to cite this article: MEI Yu, ZHANG Ping, YAN Yingwen. Numerical simulation on spray characteristics of fuel jet in a crossflow[J]. Transactions of Nanjing University of Aeronautics and Astronautics, 2020, 37(S): 18-27.

http://dx.doi.org/10.16356/j.1005-1120.2020.S.003

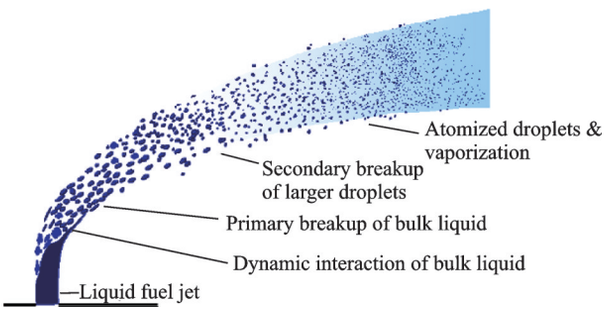

Fig.1 Schematic of liquid jet breakup and vaporization in a gas crossflow

nuities for pressure, density and viscosity. Coupling the volume of fluid (VOF) and level set methods has been proved to be very efficient for mass conservation in 2D and 3D test cases. Duarte et al.[6] used a mathematical, numerical and computational model to investigate the primary atomization of a turbulent liquid jet in crossflow. A comparison between the standard VOF method and the fine grid volume tracking (FGVT) method was reported. The model was validated against experimental correlations for the liquid jet column trajectory, and the droplet size distribution was compared to a previous numerical study from the literature. In addition, the breakup mechanisms predicted were qualitatively compared to those in previous reports. The results of the liquid column trajectory from the simulations performed presented low differences with the literature for both methods tested. According to the numerical results obtained from the computational simulations, the liquid column trajectory was well captured and the droplet size distribution was similar to the literature.

As for secondary breakup, Liu et al.[7] studied the atomization process of liquid jet in a supersonic crossflow by the Euler-Lagrangian method, in which the governing equation of the gas phase is the three-dimensional Navier-Stokes (N-S) equation in the Euler-framework, and the liquid phase adopts the Lagrangian orbit model. A new hybrid Kelvin-Helmholtz (K-H) and Rayleigh-Taylor (R-T) atomization model was used to describe the atomization process. However, only the secondary breakup process of large droplet breakage can be obtained, and the primary breakup process, in which the liquid column is broken into large droplets, cannot be simulated. Zhang et al.[8] performed numerical simulation of the secondary breakup of droplets based on the SIMPLE scheme and used the VOF method, coupled with the level-set method, to capture the boundary. They obtained the four droplet breakup regimes in secondary breakup: bag-regime, bag-plume regime, plume-sheet thinning regime, sheet thinning regime. With the increase of the *We* number, the wavelength of the unstable surface wave on the surface of droplet also increases. As the wavelength increases, the fracture mode gradually transforms from a packet to a layer. Young et al.[9] used the hybrid wave breakup model to simulate the liquid column and droplet breakup process, and analyzed the penetration depths and sauter mean diameter (SMD) distribution of the momentum ratio and the temperature change of the ambient gas flowing downstream. The SMD distribution was similar to Stenzler's[10] experimental results, especially the location of the atomization core, which was in good agreement. The SMD distribution was similar to the distribution in Stenzler's experimental results, especially in the spray core location.

The liquid fuel is injected at an angle that is perpendicular or approximately perpendicular to the direction of the gas flow and then atomized. This is a common spray atomization method in engines due to its simplicity, so this representative atomization method has been investigated in-depth by researchers at home and abroad. Liu et al.[11] used TAB model and Reitz wave instability model, and the influence of different experience parameters of these two models were analyzed for reference. By comparing the simulation results with experimental ones, both of these two models could give correct penetration, but TAB model could also provide better liquid distribution than Reitz wave model, as well as SMD and liquid droplets velocity.

Some scholars summarize the empirical formulas through experimental methods to study the spray characteristics of liquid jet in a crossflow. Jacob et al.[10] conducted experiments on the atomization of liquid jet in a cross flow. The experiments were conducted in an atmospheric pressure facility at air ve-

locity up to 110 m/s and air temperature up to 300 ℃ using distilled water, acetone, and 4-heptanone as test liquids. The droplet size and droplet trajectory have been obtained using several empirical formulas to predict the effect of liquid viscosity, the momentum ratio and the gas Weber number on liquid atomization. Wu et al.[12] used a phase doppler particle anemometry (PDPA) to experimentally study the flow pattern of a liquid jet injected into a subsonic lateral airflow spray. The SMDs on different cross sections were obtained and the relationship between the atomization characteristic parameters and the momentum ratio was summarized. Bellofiore et al.[13] studied the atomization of the liquid jet in the crossflow by experiment. Changing the speed of liquid and air, liquid properties, air pressure and temperature to explore the main features of atomization phenomenon. It was found that the jet trajectory was independent of the liquid type and could be well described by a power function. The position coordinates of the column breakup point (CBP) were related to some dimensionless parameters (such as momentum ratio, Reynolds number, Weber number, etc.). Sheng et al.[14] carried out experiments about atomization process of the annular jet in the crossflow, and captured the transient process of the annular jet liquid film breakup and atomization in the crossflow by high-speed photography. Results showed that the annular jet can achieve stable atomization in the lateral airflow. And the atomization morphology under different experimental conditions was analyzed, and the dimensionless correlation of the jet trajectory was given.

Although great efforts were made to develop a hybrid model for the primary and secondary breakups, few of them has been applied to practical issues.

Here, the coupled volum of fluid discrete phase model (VOF-DPM) method in Fluent was used to simulate the entire atomization process of a kerosene jet in the crossflow. The structural morphology and spray characteristics were obtained and analyzed using different coupling strategies. The coupling strategies involved were described as:

Case 1 Triggering the coupled VOF-DPM model on the basis of a fully developed volume fraction field.

Case 2 Simultaneously triggering the VOF method and DPM method.

Case 3 Considering the secondary breakup model while using the coupled model.

1 Numerical Methods

1.1 VOF method

The VOF model can model two or more immiscible fluids by solving a single set of momentum equations and tracking the volume fraction of each of the fluids throughout the domain.

The tracking of the interface(s) between the phases is accomplished by the solution of a continuity equation for the volume fraction of one (or more) of the phases. For the qth phase, this equation has the following form

$$\frac{1}{\rho_q}\left[\frac{\partial}{\partial t}(\alpha_q\rho_q)+\nabla\cdot(\alpha_q\rho_q\boldsymbol{v}_q)=S_{\alpha_q}+\sum_{p=1}^{n}(\dot{m}_{pq}-\dot{m}_{qp})\right] \tag{1}$$

where $\dot{m}_{qp}$ is the mass transfer from phase q to phase p and $\dot{m}_{qp}$ is the mass transfer from phase p to phase q. By default, the source term on the right-hand side of Eq.(1), S_{α_q} is zero. The volume fraction equation will not be solved for the primary phase; the primary-phase volume fraction will be computed based on the following constraint

$$\sum_{q=1}^{n}\alpha_q=1 \tag{2}$$

1.2 Discrete phase model

The discrete phase method is suitable for tracking the motion of particles in secondary breakup. The method considers that a continuously distributed component occupies the entire space and can be directly described by the N-S equation. The method considers that a continuously distributed component occupies the entire space and can be directly described by the N-S equation; the other component is discretely distributed in space, and its motion is determined by the transport equation of the continuous fluid.

The gas phase in the crossflow is treated as a

continuous phase. The following continuity equation and energy conservation equation are governing equations

$$\frac{\partial \alpha_g \rho_g}{\partial t} + \nabla \cdot (\alpha_g \rho_g U_g) = 0 \tag{3}$$

$$\frac{\partial (\alpha_g \rho_g U_g)}{\partial t} + \nabla \cdot (\alpha_g \rho_g (U_g \otimes U_g)) - \nabla \cdot (\alpha_g \rho_g \tau_g) = -\alpha_g \nabla p_g + \alpha_g \rho_g g - F = 0 \tag{4}$$

A particle orbit tracking model was used for the liquid phase. The motion of the droplets can be described by the following equation

$$m_P \frac{d\boldsymbol{u}_P}{dt} = m_P \frac{\boldsymbol{u} - \boldsymbol{u}_P}{\tau_r} + m_P \frac{\boldsymbol{g}(\rho_P - \rho)}{\rho_P} + \boldsymbol{F} = 0 \tag{5}$$

where m_P is the mass of the particles, ρ and u are the velocity and density of the continuous phase, ρ_P and $\boldsymbol{u}_P$ are the discrete phase velocity and density. $\boldsymbol{F}$ is the joint force of extra force (virtual mass force, lift, etc.). τ_r is the relaxation time of the particle, which is defined as

$$\tau_r = \frac{\rho_P d_P^2}{18\mu} \cdot \frac{24}{C_d Re} \tag{6}$$

where μ is the molecular viscosity of the continuous phase, d_P is the particle diameter, Re is the relative Reynolds number, C_d is the coefficient of drag between the droplet and the gaseous phase. If the droplet is considered to be a smooth sphere, then C_d is defined as follows

$$C_d = a_1 + \frac{a_2}{Re} + \frac{a_3}{Re^2} \tag{7}$$

In the Eq. (7), a_1, a_2, and a_3 are constants, which are depends on Re, given by Morsi[15]. Since the density of the gas phase is much smaller than the density of the liquid phase, the force generated by the pressure gradient and the virtual mass force are negligible, so F is considered to equal 0 in the calculation.

1.3 Secondary breakup model

The Taylor analogy breakup (TAB) model is a classic method for calculating droplet breakup, which is applicable to many engineering sprays. This method is based on Taylor's analogy[16].

The TAB model was applied to numerical simulation of secondary breakup, which is based on the similarity between the oscillating deformation of the droplet and the spring mass system. The restoring force of the spring is similar to the surface tension; the aerodynamic force is similar to the external force on the mass system, and the damping force is similar to the viscosity of the liquid. Therefore, the forced harmonic equation is established.

$$m\ddot{x} = F_a - Kx - d_a \dot{x} \tag{8}$$

where m is the mass of the droplet, x the distance from the balanced position to the leading edge of the droplet. $\dot{x}$ and $\ddot{x}$ are the first derivative and second derivative of x. F_a is the influence of aerodynamic force, K the influence of surface intension, and d_a is related to the the viscosity of the liquid.

The resulting TAB model equation set, which governs the oscillating and distorting droplet, can be solved to determine the droplet oscillation and distortion at any given time. The droplet oscillations grow to a critical value the "parent" droplet will break up into a number of smaller "child" droplets.

1.4 Coupled VOF-DPM

During the primary breakup, the initial jet morphology and disintegration are predicted using the VOF method on a sufficiently fine mesh. The continuous liquid jet undergoes a strong shearing force, which leads to the column fragmenting into shreds and ligaments. Meanwhile, a mode transformation phenomenon occurs, where the liquid lump separated from the liquid core is converted into discrete Lagrangian particles if the liquid lump satisfies the lump size criteria and asphericity criteria. Then, these particles are removed from the resolved liquid in the Euler field to Lagrangian framework. Simultaneously, the spatial distribution of particle diameter, velocity, and location are obtained. Further, secondary breakup of liquid droplets will be simulated using the discrete phase model, where these structures are further disintegrated into small droplets.

1.5 Adaptive mesh refinement

The adaptive mesh refinement in Fluent allows us to modify the dense distribution and the direction of the mesh based on the results of the data calculation. Therefore, using adaptive mesh can reduce the amount of mesh and ensure the calculation accuracy. In this paper, the numerical simulation uses adaptive mesh. The effect of the adaptive mesh is shown in Figs.2, 3.

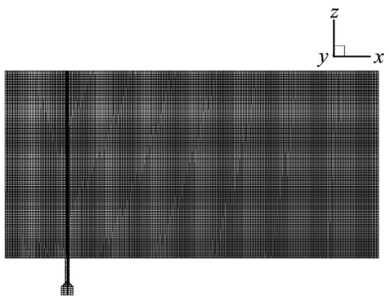

Fig.2 Initial mesh

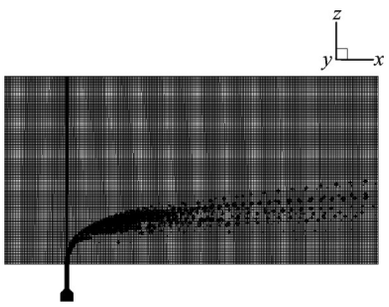

Fig.3 Adaptive mesh

Grid adaption is based on the iteration of time step. The size of the basic thus have a large impact on the calculation results.

2 Computational Domain and Boundary Conditions

Plain orifice injector is widely used in aircraft engines to create a liquid jet spreading into a cross flow. The schematic diagram of the plain orifice injector used in experiments[17] is shown in Fig.4. The diameter of the injector orifice is 0.4 mm, and the transition between the orifice and the fuel tube is a 90° cone.

The computational domain is shown in Fig.5, which measures 36 mm × 4.8 mm × 18 mm. The origin of coordinate system is located in the center of the orifice. The fuel velocity is along the direction z and the air velocity is along the x direction. Mesh model with 1.73 million structured grids was obtained in Gambit and the initial grid scale is 125 μm. Using the adaptive mesh refinement technique, the smallest grid in the liquid domain can reach 25 μm, which enables the capture of small-scale liquid structures in the atomization process.

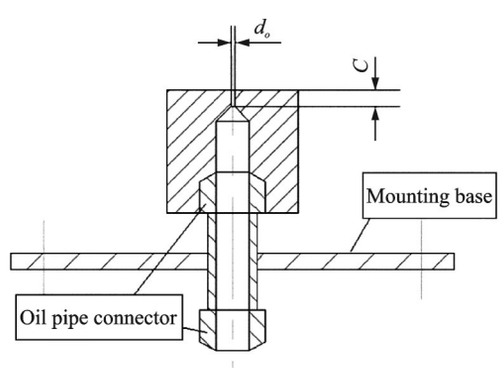

Fig.4 Schematic diagram of the plain orifice injector

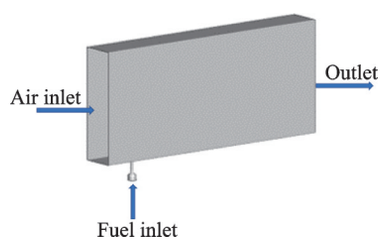

Fig.5 Boundary conditions

The fluid properties and computational conditions are shown in Table 1, which are consistent with the operating conditions in experiments.

Table 1 Fluid properties and computational conditions

Parameter	Value
Liquid density/(kg·m^{-3})	780
Air density/(kg·m^{-3})	1.225
Liquid velocity/(m·s^{-1})	12
Air velocity/(m·s^{-1})	90
Surface tension/(N·m^{-1})	0.026
Momentum flux ratio	16
Weber number	167.9

3 Results and Discussion

3.1 Flow field structure and jet morphology

The gas velocity distributions of plane y=0 is shown in Fig.6. It can be seen from the velocity profile that there was a significant velocity recirculation

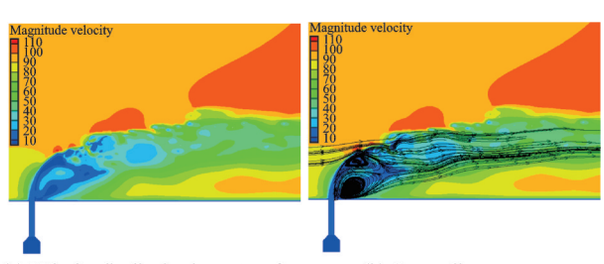

(a) Velocity distribution in contour form (b) Streamline pattern

Fig.6 Velocity distribution at plane y=0

zone on the leeward side of the liquid column due to the kerosene jet. After ejected from the orifice into a high-speed cross flow, the initial direction of the liquid jet is along the z-coordinate, and a direction deflection occurred under the pressure of aerodynamic force, leading to the bend of liquid column. Therefore, a recirculation is produced in the leeward side.

The evolution of iso-surface that volume fraction equals 0.1, as shown in Fig.7. After the fuel injected from the injector exit, the liquid column is inclined to the airflow direction under the pressure of aerodynamic force and gradually spreads out along the y direction. Owing to a strong shearing interaction between air and fuel, the jet tends to fluctuate on the surface, further leading to the detachment of small liquid ligaments from the liquid column. Finally, these ligaments are disintegrated into lots of small droplets.

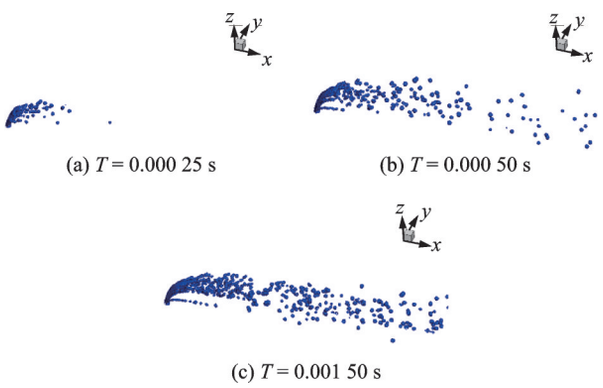

Fig.7 Evolution of iso-surface of volume fraction being 0.1

3.2 Time-average SMD distribution

After a fully developed volume fraction field of the liquid phase was obtained, some small liquid lump is transformed into discrete phase particles in the Lagrangian framework by VOF-DPM method. Then the spatial distribution characteristics of the droplets are obtained. Using postprocess method, the time-average SMD spatial distribution and the particle size distribution of the spray were obtained, as shown in Fig.8.

The time-average SMD distribution and spatial distribution of fuel droplets measured by experiment is shown in Fig.9. In terms of the particle distribution, along the flow direction of air, the droplets have a tendency to decrease in size. Owing to the strong gas-liquid shear stress, the droplets are

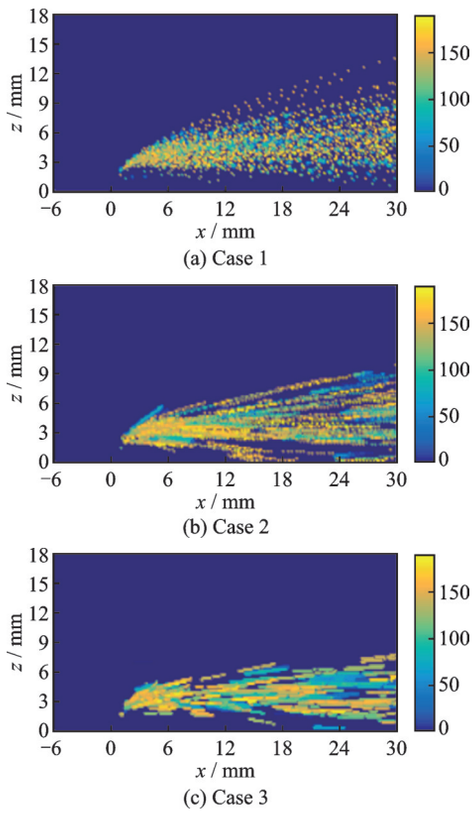

Fig.8 Time-averaged SMD distribution

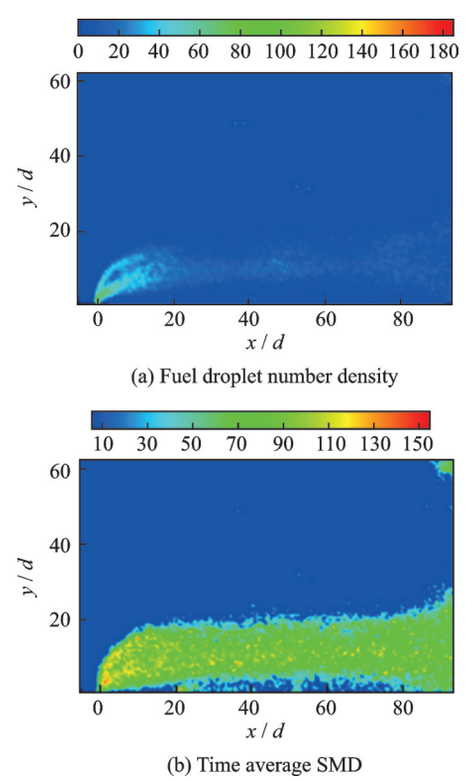

Fig.9 Droplet number density and time average SMD

relatively smaller on the surface of liquid column, while larger in the jet core. Compared the numerical results with experimental data, it suggested that the numerical SMD distribution agreed well ith the experimental results. The time-averaged SMD distributions obtained using different coupling strategies suggested that Case 1, where the coupled VOF-DPM model was launched on the basis of a fully developed volume fraction field, performed better in the prediction of the spray distribution.

3.3 Jet trajectory

The schematic of the experimental equipment for measurement of the jet trajectory was shown in Fig. 10. The LED light was used to illuminate the droplets and the camera to collect the jet trajectory from the side of the injector.

The spray distribution in the simulation and the outline of jet trajectory measured in the experiments are presented in Fig.11. The time-average spray distribution obtained by postprocessing in simulation is shown in the left column of Fig.11 and the instantaneous spray distribution is in the right column. In terms of the jet trajectory, there is a slight difference between the numerical and experimental results. In the vicinity of injector exit, the spray distribution is within a range of the trajectory outline. With increase of the distance from the exit, the penetration depth increases and the spray distribution range enlarges, which even exceeds the distribution range in experiments. Compared the spray distribution using different coupling strategies, Case 1 has the best performance. And the difference between Case 3 and the experimental data is larger than the other two cases.

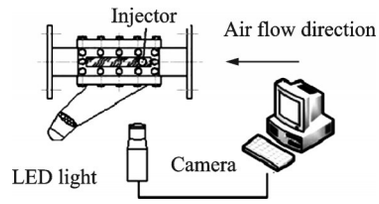

Fig.10 Schematic of experimental equipment

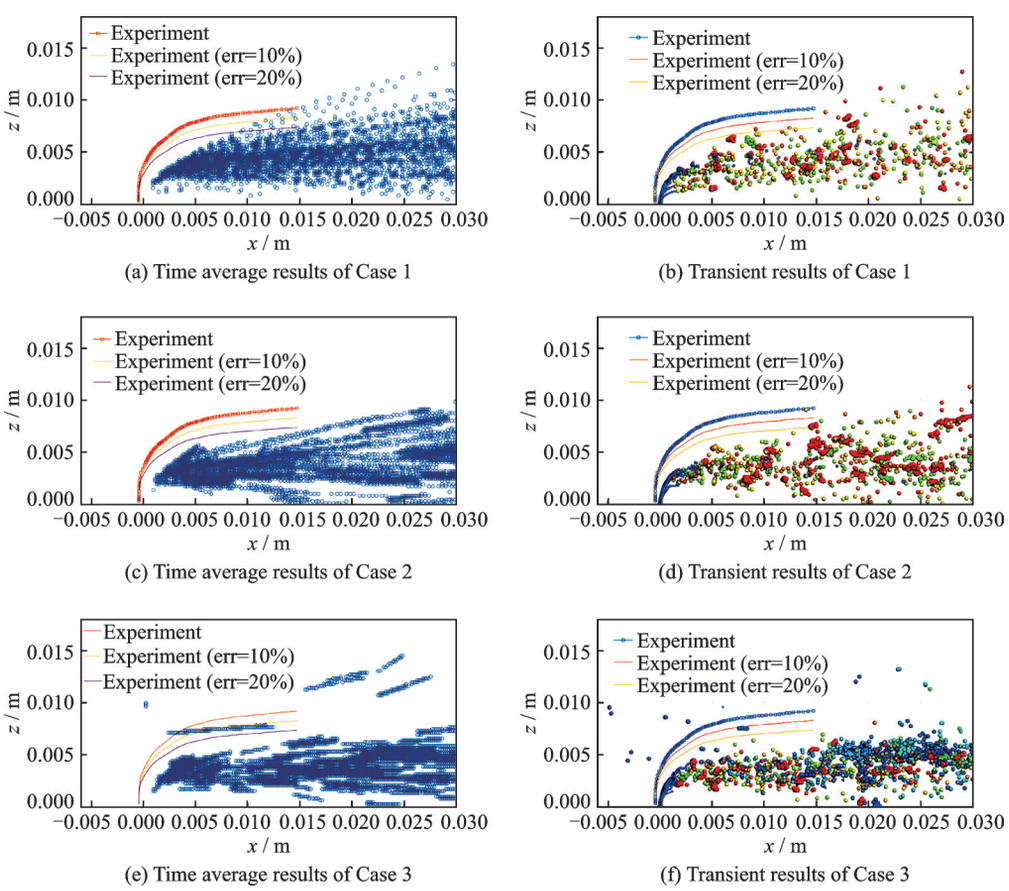

(a) Time average results of Case 1 (b) Transient results of Case 1

(c) Time average results of Case 2 (d) Transient results of Case 2

(e) Time average results of Case 3 (f) Transient results of Case 3

Fig.11 Comparison of jet trajectory in simulation and experiments (d=0.4 mm, We=167.9, q=16.0)

To further validate the numerical results, two typical correlations of jet trajectories previously proposed by others were applied as Refs.[11-12].

$$\text{Wu: } \frac{y}{d} = 1.37\left(q\frac{x}{d}\right)^{0.5} \tag{9}$$

$$\text{Stenzler: } \frac{y}{d} = 2.63q^{0.442}\left(\frac{x}{d}\right)^{0.39} We^{-0.088}\left(\frac{\mu}{\mu_{h_2o}}\right)^{-0.027} \tag{10}$$

Comparisons between the numerical results and two correlations are shown in Fig.12. It suggests that the numerical results agree well with the correlation offered by Stenzler, while differ from Wu's statistical results. The main reason is that Wu did not consider the influence of We on the jet trajectory, which indicates that the effect of We cannot be ignored. Moreover, Case 1 and Case 2 perform better than Case 3 compared with the correlations.

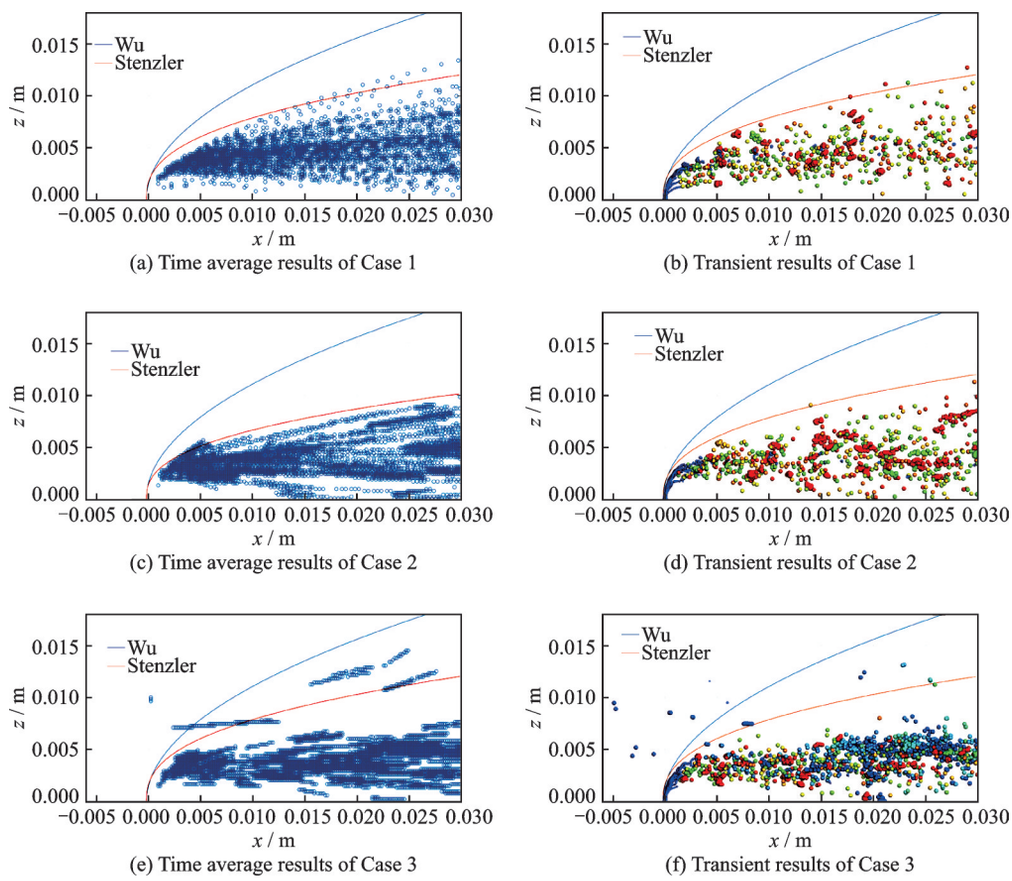

Fig.12 Comparisons of jet trajectory between numerical results and correlations (d=0.4 mm, We=167.9, q=16.0)

3.4 Column breakup point

The column breakup point is defined as the position where the core area of the liquid column enters a more detailed atomization stage. It is the critical point between the core region of the liquid column and the discrete phase mechanism.

The instantaneous spray distribution consists of the continuous liquid phase and the lagrangian discrete particles was obtained. The breakup point in simulations are considered to be located in the point where the breakup phenomena extensively occurs on the liquid column. The results using different coupled strategies are shown in Fig.13.

The locations of column breakup point simulated in three cases are slightly different, which is nearly situated in the x coordinate ranging from $6d$ to $7d$ and in the z coordinate ranging from $8.5d$ to $9d$ (d is the diameter of the injector orifice). The coupled strategies have few effects on the column breakup point. Compared with the correlations, the column point has a divergency. The numerical results are smaller both in x and y coordinates. The main reason is that different fluids are used in the simulation and experiments. It suggests that the fluid properties

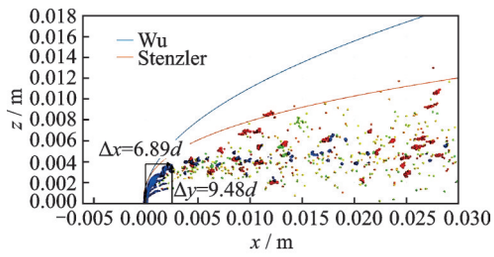

(a) Case 1 (d=0.4 mm, q=16, We=167.9)

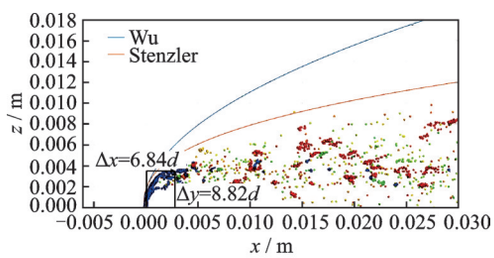

(b) Case 2 (d=0.4 mm, q=16, We=167.9)

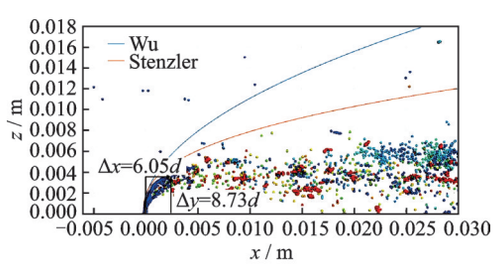

(c) Case 3 (d=0.4 mm, q=16, We=167.9)

Fig.13 Column breakup points

influence the breakup point.

4 Conclusions

Different coupled VOF-DPM strategies are applied to simulate the atomization process of kerosene jet in crossflow through the plain orifice injector. By comparing the numerical calculation results with experimental one and the empirical formula.

(1) Case 1 (Triggering the coupled VOF-DPM model on the basis of a fully developed volume fraction field.) behave best at the simulation of fuel jet in a crossflow.

(2) While the VOF-DPM model was used, TAB model has a negative impact on the simulation accuracy.

(3) The effect of We cannot be ignored when summarizing the correlations of jet trajectories.

References

[1] HOU L Y, HOU X C. Nozzle technical manual[M]. Beijing: China Petrochemical Press, 2002. (in Chinese)

[2] PEI K, WU K. Breakup processes of liquid jets in subsonic crossflows[J]. Journal of Propulsion & Power, 1997, 13(1): 64-73.

[3] HIRT C W, NICHOLS B D. Volume of fluid (VOF) method for the dynamics of free boundaries[J]. Journal of Computational Physics, 1981, 39(1): 201-225.

[4] BRINCKMAN K W, HOSANGADI A, AHUJA V, et al. A CFD methodology for liquid jet breakup and vaporization predictions of compressible flows[C]//Proceedings of the 46th AIAA Aerospace Sciences Meeting. Reno, Nevada: AIAA, 2016.

[5] MÉNARD T, TANGUY S, BERLEMONT A. Coupling level set/VOF/ghost fluid methods: Validation and application to 3D simulation of the primary break-up of a liquid jet[J]. International Journal of Multiphase Flow, 2007, 33(5): 510-524.

[6] DUARTE B A D F, BARBI F, VILLAR M M. Primary atomization of a turbulent liquid jet in crossflow: A comparison between VOF and FGVT methods[J]. Journal of the Brazilian Society of Mechanical Sciences and Engineering, 2020, 42(6): 1-13.

[7] LIU J, WANG L, ZHANG J. Experimental and numerical simulation of atomization of liquid jet in supersonic crossflow[J]. Journal of Aerospace Power, 2008, 23(4): 724-729. (in Chinese)

[8] ZHANG Y S, XUE L P. Numerical simulation of droplet breakup regimes in secondary atomization[J]. Chinese Quarterly of Mechanics, 2015, 36(4): 574-585. (in Chinese)

[9] YOUNG L Y, DOO H H, JI S H, et al. A large eddy simulation of the breakup and atomization of a liquid jet into a cross turbulent flow at various spray conditions[J]. International Journal of Heat and Mass Transfer, 2017,112(9): 97-112.

[10] JACOB N S, JONG G L, DOMENIC A S. Penetration of liquid jets in a crossflow[J]. Atomization and Sprays, 2006,16: 887-906.

[11] LIU J, XU X. Application on numerical simulation of atomization of liquid jet in crossflow using two atomization models[J]. Journal of Aerospace Power, 2013, 28(7): 1441-1448. (in Chinese)

[12] WU P K, FULLER R P, KIRKENDALL K A. Spray structures of liquid jets atomized in subsonic Crossflows[J]. Journal of Propulsion and Power, 1998, 14: 173-182.

[13] BELLOFIORE A, CAVALIERE A, RAGUCCI R. Air density effect on the atomization of liquid jets in crossflow[J]. Combustion Science and Technology, 2007, 179(1): 319-342.

[14] SHENG G H, ZHANG H B, ZHAO Z C. Breakup and atomization of annular flow jet in crossflow[J]. Journal of University of Chinese Academy of Sciences, 2017, 34(2): 160-165.
[15] MORSI S A. An investigation of particle trajectories in two-phase flow systems[J]. Fluids Mech, 1972, 55(2): 193-208.
[16] TAYLOR G I. The shape and acceleration of a drop in a high speed air stream[J]. Scientific Papers, 1963, 3: 457-464.
[17] DANG L F. Research on fuel atomization and evaporation of primary swirler in a LPP combustor[D]. Nanjing: Nanjing University of Aeronautics and Astronautics, 2014. (in Chinese)

Acknowledgement This work was supported by the National Natural Science Foundation of China (No. 91741118).

Authors Mr. **MEI Yu** received his bachelor's degree in mechanical engineering from Nanjing University of Aeronautics and Astronautics in 2018. Since 2018, he has been studying for his master's degree in Nanjing University of Aeronautics and Astronautics. His research is focused on atomization and atomizer.

Prof. **YAN Yingwen** is a professor and doctoral supervisor of Nanjing University of Aeronautics and Astronautics. His research focuses on atomization and atomizer, low emission combustion, thermo-acoustic instabilities, and chemical reaction kinetics.

Author contributions Mr. **MEI Yu** designed this study, conducted the analysis, interpreted the results and wrote most of the manuscript. Ms. **ZHANG Ping** contributed to the discussion and background of the study. Prof. **YAN Yingwen** checked the manuscript. All authors commented on the manuscript draft and approved the submission.

Competing interests The authors declare no competing interests.

(Production Editor: ZHANG Tong)

横向射流中煤油雾化过程的数值模拟

梅　雨，张　萍，颜应文

(南京航空航天大学能源与动力学院，南京 210016，中国)

摘要：对航空煤油经直射喷嘴喷入横向射流的雾化过程进行数值研究，采用VOF多相流计算模型、DPM离散相模型和TAB二次雾化模型，应用动态网格自适应技术。采用不同的VOF-DPM耦合方式，模拟了一定韦伯数和动量比下煤油喷入横向气流中雾化过程的射流破碎形态及发展轨迹，获得了雾化后油滴的SMD空间分布和油滴轨迹。与实验结果和经验公式比较后，验证了所采用不同计算方法的合理性。

关键词：直射式喷嘴；初次雾化；二次雾化；射流轨迹；SMD